2018-12

MORPHODYNAMIC CLASSIFICATION OF COASTAL REGIONS USING DEEP LEARNING THROUGH DIGITAL IMAGERY COLLECTION

Herrmann, David W.

Monterey, CA; Naval Postgraduate School

NAVAL POSTGRADUATE SCHOOL

MONTEREY, CALIFORNIA

THESIS

MORPHODYNAMIC CLASSIFICATION OF COASTAL REGIONS USING DEEP LEARNING THROUGH DIGITAL IMAGERY COLLECTION

by

David W. Herrmann

December 2018

Thesis Advisor:	Mara S. Orescanin
Second Reader:	Derek Olson

THIS PAGE INTENTIONALLY LEFT BLANK

REPORT DOCUMENTATION PAGE			*Form Approved OMB No. 0704-0188*

1. AGENCY USE ONLY *(Leave blank)*	**2. REPORT DATE** December 2018	**3. REPORT TYPE AND DATES COVERED** Master's thesis

4. TITLE AND SUBTITLE MORPHODYNAMIC CLASSIFICATION OF COASTAL REGIONS USING DEEP LEARNING THROUGH DIGITAL IMAGERY COLLECTION	**5. FUNDING NUMBERS**
6. AUTHOR(S) David W. Herrmann	
7. PERFORMING ORGANIZATION NAME(S) AND ADDRESS(ES) Naval Postgraduate School Monterey, CA 93943-5000	**8. PERFORMING ORGANIZATION REPORT NUMBER**
9. SPONSORING / MONITORING AGENCY NAME(S) AND ADDRESS(ES) N/A	**10. SPONSORING / MONITORING AGENCY REPORT NUMBER**

11. SUPPLEMENTARY NOTES The views expressed in this thesis are those of the author and do not reflect the official policy or position of the Department of Defense or the U.S. Government.

12a. DISTRIBUTION / AVAILABILITY STATEMENT Approved for public release. Distribution is unlimited.	**12b. DISTRIBUTION CODE** A

13. ABSTRACT (maximum 200 words)

The DoD is investing in autonomy, AI, and machine learning. Deep learning, a sub-field of machine learning is increasing due to newer and cheaper hardware, new algorithms, and big data. Deep learning uses a neural network with multiple weighted layers designed to learn hierarchical feature representations. This research uses the technique of transfer learning, which takes the well-constructed architecture of a source model and retrains it to a target data set—in this case, different coastal landscapes. Eight different classes were trained with oblique (≥ 45°) images. An average accuracy of 95% correct identification was achieved through validation testing. Carmel River State Beach is a known morphodynamic site that changes seasonally. Five different stitched together <10° off NADIR mosaics of this site were selected to test the model's ability to detect and correctly label areas of change over time. The mosaics were broken into four quadrants of equal area to increase homogeneity of the features. The two landward quadrants showed successful label and change detection; the seaward quadrants showed poor results attributed to smearing and gradient distortion from the stitching process. Successful transfer learning was accomplished with high accuracy; angle differences and stitching caused mislabeling. Larger datasets with single images from multiple angles may reduce labeling error. Multi-label and multispectral approach will enhance and broaden the application of this process..

14. SUBJECT TERMS machine learning, neural networks, coastal landscape, coastal imagery, remote sensing, data processing, artificial intelligence, deep learning	**15. NUMBER OF PAGES** 65
	16. PRICE CODE

17. SECURITY CLASSIFICATION OF REPORT	**18. SECURITY CLASSIFICATION OF THIS PAGE**	**19. SECURITY CLASSIFICATION OF ABSTRACT**	**20. LIMITATION OF ABSTRACT**
Unclassified	Unclassified	Unclassified	UU

THIS PAGE INTENTIONALLY LEFT BLANK

Approved for public release. Distribution is unlimited.

MORPHODYNAMIC CLASSIFICATION OF COASTAL REGIONS USING DEEP LEARNING THROUGH DIGITAL IMAGERY COLLECTION

David W. Herrmann
Lieutenant Commander, United States Navy
BS, Wilkes University, 2003
MS, Thomas Jefferson University, 2006

Submitted in partial fulfillment of the
requirements for the degree of

MASTER OF SCIENCE IN METEOROLOGY AND PHYSICAL OCEANOGRAPHY

from the

NAVAL POSTGRADUATE SCHOOL
December 2018

Approved by: Mara S. Orescanin
Advisor

Derek Olson
Second Reader

Peter C. Chu
Chair, Department of Oceanography

THIS PAGE INTENTIONALLY LEFT BLANK

ABSTRACT

The DoD is investing in autonomy, AI, and machine learning. Deep learning, a sub-field of machine learning is increasing due to newer and cheaper hardware, new algorithms, and big data. Deep learning uses a neural network with multiple weighted layers designed to learn hierarchical feature representations. This research uses the technique of transfer learning, which takes the well-constructed architecture of a source model and retrains it to a target data set—in this case, different coastal landscapes. Eight different classes were trained with oblique (≥ 45°) images. An average accuracy of 95% correct identification was achieved through validation testing. Carmel River State Beach is a known morphodynamic site that changes seasonally. Five different stitched together <10° off NADIR mosaics of this site were selected to test the model's ability to detect and correctly label areas of change over time. The mosaics were broken into four quadrants of equal area to increase homogeneity of the features. The two landward quadrants showed successful label and change detection; the seaward quadrants showed poor results attributed to smearing and gradient distortion from the stitching process. Successful transfer learning was accomplished with high accuracy; angle differences and stitching caused mislabeling. Larger datasets with single images from multiple angles may reduce labeling error. Multi-label and multispectral approach will enhance and broaden the application of this process.

THIS PAGE INTENTIONALLY LEFT BLANK

TABLE OF CONTENTS

LIST OF FIGURES

LIST OF ACRONYMS AND ABBREVIATIONS

AWS	Amazon Web Services
CNN	Convolutional Neural Network
CRSB	Carmel River State Beach
DJI	Da Jiang Innovations
DoD	Department of Defense
EC2	Elastic Compute Cloud (Amazon EC2)
GIS	Geographic Information System
GPU	Graphics Processing Unit
NOAA	National Oceanic and Atmospheric Administration
ReLU	Rectified Linear Unit
UASs	Unmanned Aerial Systems
VGG19	Visual Geometry Group's 19

THIS PAGE INTENTIONALLY LEFT BLANK

ACKNOWLEDGMENTS

I would like to express my great appreciation to Dr. Mara Orescanin for being my advisor and allowing me to complete my master's thesis under her guidance. I am grateful for the numerous hours she spent working with me and her patience in getting me through this process on the emerging topic of machine learning. This thesis would not have been possible without her critical feedback and counsel; she was there every step of the way. To my second reader, Dr. Derek Olson, I appreciate his keen eye to detail and the exceptional critiques that took this thesis to the next level. His perspective shed light on areas where I would have come up short. Thank you for your time and dedication.

To the Naval Postgraduate School professors and staff in the Meteorology and Oceanography departments, thank you. Your dedication to the students is seen every day through your work ethic and willingness to go the extra mile to see us succeed. The Navy will reap the rewards of your efforts for many years to come.

To my NPS cohort, you all hold a special place in my heart. You have made a positive impact on me, and I could not have asked for a better group to take on this journey. Everyone at one point or another helped me with my studies, and I am truly grateful for your patience and assistance. I wish all of you success in the Navy and your personal journeys and hope we will meet again.

Lastly, to my wife, Jessie, and daughter, Morgan: Jessie, you have always been there for me, showing unwavering support. Your daily sacrifices are testament to your commitment as a great wife, mother, and best friend. Through thick and thin, you were there. Morgan, since you came into my life a little less than two years ago, I always have a smile on my face. After a busy day, coming home to see the smile on your face brings me so much joy. My success is the direct result of the love and dedication you provide me.

THIS PAGE INTENTIONALLY LEFT BLANK

I. MOTIVATION

The rapid advancement of technology, along with its wide distributed availability, has enabled our adversaries to level the playing field in terms of fighting a modern war. In recognition of this, the Department of Defence (DoD) is investing heavily in autonomy, artificial intelligence, and machine learning to gain the military advantages the United States needs to remain competitive (Mattis 2018). Specifically, for the U.S. Navy, the open ocean's more static environment is a much lesser a concern than the coastal and more confined regions of operation. These littoral regions are morphodynamic, and features can change rapidly causing difficulty in modeling and forecasting. It is my job as a naval meteorology and oceanography officer to understand these environments and produce high quality products for commanders to make critical decisions.

The aim of this study is to use machine learning, specifically, neural networks to develop a process for high accuracy and rapid classification of images taken from an unmanned aerial systems (UASs) of various coastal attributes and accurately detect coastal morphological change. It has been shown that coastal areas with ephemeral river outflow cause water circulation changes and massive sediment transport drastically changing the beach structure (Orescanin and Scooler 2018; Young 2018). It is important that we have a method to detect and analyze these features for U.S. naval amphibious operations. This is extremely important for insertion, and extraction of small special operations teams whose missions often do not have long leeway for planning and where accurate environmental intelligence is critical.

THIS PAGE INTENTIONALLY LEFT BLANK

II. INTRODUCTION

In recent years, the advancement of technology and its affordability has enabled the remote sensing field to rapidly expand. The use of remote sensing to detect coastal environmental change is a unique problem, especially relevant to the U.S. Navy and Marine Corps. A changing coastline affects many areas, such as zoning concerns with regard to hazards, coastal erosion and accretion prediction and studies, where to build setbacks, sediment budgets and difficulties in coastal morphodynamic modeling all occur (Sherman and Bauer 1993; Al Bakri 1996; Zurek et al. 2003; Maiti and Bhattacharya 2009).

Another result of this advancing technology is the vast amount of imagery data collected. In recent years, the dataset and diversity of coastal photographic imagery has grown immensely, this is partly due to an increase in coastal camera stations and improvements in resolution and digital data storage capacity (Hoonhut et al. 2015). Traditional means of collecting data through manned aircraft and satellite often do not have the resolution, cost, or flexibility that unmanned aircraft systems (UASs) can provide (Hugenholtz and Whitehead 2014). New improvements of sensors and resolution, as well as, development of small (<15kg) UASs that are more versatile and easily accessible for civil, commercial, and scientific use provide the means to capture high resolution imagery safely from lower altitudes, further increasing the volume of coastal imagery datasets (Whitehead 2014).

This huge influx of coastal imagery creates a new dilemma regarding how best to analyze, classify, and quantify it. The amount of human resources and man-hours of analysis to interpret this data will not only be time consuming but costly and subjective as well. A better way to engage this problem is to use machine learning, specifically the subcategory within it called deep learning. Machine learning is a process, where trained automated system searches for useful representations of some input data that is within a predefined space of possible outcomes using guidance from a feedback mechanism (Chollett2018). The deep learning, specifically convolutional neural networks, subcategory dives in further by exposing the machine to a representative input data set. Deep learning uses successive layers (Figure 1, right) of increasingly meaningful data representations

during the learning process, through a series of interconnected neurons. Each neuron specializes in feature extraction, and is a tunable parameter within the overall model architecture. Given the large number of tunable parameters, it is critical to have sufficiently large datasets (usually thousands of images) to create the best optimization of these parameters. These methods can often deliver highly accurate classification results, especially when using a large representative training data set (Marmanis et al. 2015 and Chollett 2018).

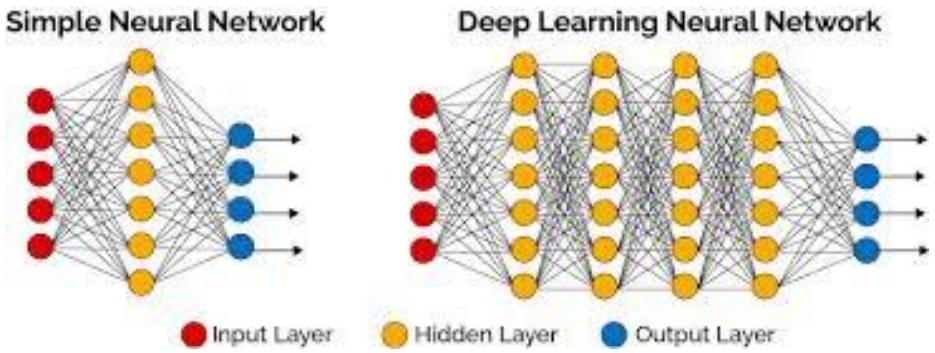

Figure 1. Comparison of a simple neural network and the increased layers of a deep learning network. Source: Quora (2018).

Machine learning and deep neural networks have quickly become the cutting-edge technology for computer based image recognition and classification (Krizhevsky et al. 2012; Simonyan and Zisserman 2014; Han et al. 2016). Effective deep learning will produce a trained neural network that is capable of producing high accuracy (>90% correct identification) output to the target output results. This is the desired goal for high throughput classification and change identification of coastal imagery from these massive data sets.

Until recently, the primary means of high-resolution remote imaging was through the use of satellite imagery, which was mostly analyzed by a human operator. Coastal accretion and erosion, land use/cover with GIS and neural networks, and mapping of natural hazards and disasters have been extensively studied through examination of satellite imagery using various analysis techniques (Mas 2004; Joyce et al. 2009; Natesan et al.

2015). The popularity of unmanned aerial systems (UASs), along with their relatively low cost, is a commonly used tool being used to map and monitor areas of environmental interest including cropland and forestry (Johnson et al. 2003; Lelong et al. 2008; Dunford et al. 2009; Rango et al. 2009; Turner et al. 2012).

A common approach of extracting coastlines is change detection using satellite imagery. A common technique is using Landsat imagery and topographic maps over different years and creating overlays using ArcGIS to assess change detection such as in erosion, accretion and construction is well documented (Li and Damen 2010; Tamassoki et al. 2014; Ghosh et al. 2015; Kankara et al. 2015). Satellite imagery is limited by its resolution, obstacles, infrequent passes, and cloud coverage (Cermakova et al. 2016); all of these factors can be significantly mitigated when using UASs. There has been progress using UASs for change detection, specifically soil erosion in Morocco where the results where comparable with direct fieldwork attributed to the high resolution that was achieved from the UAS (d'Oleir-Oltmanns et al. 2012).

The study of coastal changes using machine-learning techniques has begun to take root recently. There are requirements and challenges that must be taken into consideration when training the neural network, especially considering the heterogeneous nature of landscape imagery. Classifying imagery is not trivial, and involves the human operator to make a decision and add a specific label to the data based on their interpretation of it. Classification process is a problem, especially when trying to assign one specific class to an image. Most imagery is not homogenous to one type of class; large images often capture multiple classes. There are key problem characteristics one must be aware of: scarcity of data, imbalanced training set, examples are naturally grouped in batches, and performance task where a classifier is used to decide which images go to humans for verification (Kubat et al. 1998). Specifically, it is imperative to have an adequate number of training samples that are representative (Hubert-Moy et al. 2001; Chen and Stow 2002; Landgrebe 2003; Mather 2004; Lu and Weng 2007). Complex heterogeneous landscapes make it difficult to select training samples that accurately represent the class. This problem is further complicated by the data's spatial resolution that may cause large volumes of mixed pixels, which are recognized as a major problem of effective use of remote sensed

data in per-pixel classifications (Fisher 1997; Cracknell 1998; Lu and Weng 2007). The technique of image segmentation addresses this issue by separating the image into homogenous regions (Kuleli et al. 2011), and merging pixels into objects (also called superpixels) that are then classified based on different objects instead of the more error prone way of classification using individual pixels (Lu and Weng 2007).

Recently an accurate hybrid segmentation method (Buscombe and Ritchie 2018), combines the ability of deep convolutional neural networks to classify small regions in an image plus the use of fully connected conditional random fields for fine-grained localization pixel-level classification. This method has achieved high accuracy classification results of 88–98% (F1 scores) for five datasets using a different number of tiles applicable to large, spatially extensive landscapes (Buscombe and Ritchie 2018) and can also be applied to large morphodynamic heterogeneous coastal areas.

In order to test, the applicability of deep learning on change detection, of coastal landscapes, over 10000 images of the U.S. coasts were hand classified into nine categories. This dataset is used to both train from scratch and to apply transfer learning using the neural network, Visual Geometry Group 19 (VGG19). Furthermore, a change detection algorithm is developed and tested at Carmel River State Beach (CRSB), CA. CRSB is a small pocket beach near the Carmel River that is known to breach during the transition to winter months **(**Figure 2). CRSB contains an ephemeral river that is periodically opened and closed to the Pacific Ocean depending on the time of year and accumulated seasonal precipitation, thus making CRSB a highly dynamic area prone to rapid coastal changes. By taking advantage of UASs, and technology the next leap forward is to take high-resolution UAS imagery and analyze it using deep neural networks. The goal being a product that is accurate and capable of identifying morphodynamic areas in the imagery through change detection.

Carmel River State Beach located just south of Monterey Bay along California's Central Coast.

Figure 2. Carmel River State Beach. Source: Scooler (2017).

The hypothesis of this study is twofold. First, it is hypothesized that heterogeneous coastal landscapes can be used to train a deep neural network through transfer learning and training from scratch with a high degree of accuracy (>90% correct identification) without the need for image segmentation. Second, it is hypothesized that high resolution UAS imagery of the same coastal site over time coupled with a trained deep neural network will be able to accurately and affectively highlight areas through change detection that varies seasonally. UASs have proven successful for mapping, surveying, and monitoring terrain. However, research using UAS imagery and deep neural networks to detect landscape change is still in its infancy. The applications of an efficient coastal landscape change detection technique is far reaching, from recreational beaches erosion and accretion, coastal construction project planning, natural disaster evaluation and relief efforts.

THIS PAGE INTENTIONALLY LEFT BLANK

III. METHODOLOGY: MODEL TRAINING, DATA COLLECTION AND ANALYSIS

A. VGG-19 MODEL ARCHITECTURE AND TRAINING

The model used for this study was Visual Geometry Group's 19 (VGG19) model, which is a 19 layer convolutional neural network that is pre-trained on millions of images from the ImageNet database, described by K. Simonyan and A. Zisserman (2014). The architecture for the VGG19 model relies primarily on convolutional layers, where 2D convolutions are performed on the input image with kernels of various sizes. These layers are known to preserve the stationarity of statistics and locality of pixel dependencies. These type of network architectures having convolutional layers are also known as Convolutional Neural Networks (CNN). Compared to standard feed-forward (fully connected) networks of similar size, CNN networks have fewer parameters making them easier to train. Additionally, linearly rectified units (ReLU) are used for neuron activations, and pooling operations are used to summarize the group of neurons in the same kernel map in non-overlapping regions (effectively reducing the size of feature maps deeper into the network). These layers (Figure 3) are applied in an alternating manner, resulting in each layer being a nonlinear filter bank with complexity increasing depending on the position of the layer in the network (Gatys et al. 2015).

Layer (type)	Output Shape	Param #
input_1 (InputLayer)	(None, 256, 256, 3)	0
block1_conv1 (Conv2D)	(None, 256, 256, 64)	1792
block1_conv2 (Conv2D)	(None, 256, 256, 64)	36928
block1_pool (MaxPooling2D)	(None, 128, 128, 64)	0
block2_conv1 (Conv2D)	(None, 128, 128, 128)	73856
block2_conv2 (Conv2D)	(None, 128, 128, 128)	147584
block2_pool (MaxPooling2D)	(None, 64, 64, 128)	0
block3_conv1 (Conv2D)	(None, 64, 64, 256)	295168
block3_conv2 (Conv2D)	(None, 64, 64, 256)	590080
block3_conv3 (Conv2D)	(None, 64, 64, 256)	590080
block3_conv4 (Conv2D)	(None, 64, 64, 256)	590080
block3_pool (MaxPooling2D)	(None, 32, 32, 256)	0
block4_conv1 (Conv2D)	(None, 32, 32, 512)	1180160
block4_conv2 (Conv2D)	(None, 32, 32, 512)	2359808
block4_conv3 (Conv2D)	(None, 32, 32, 512)	2359808
block4_conv4 (Conv2D)	(None, 32, 32, 512)	2359808
block4_pool (MaxPooling2D)	(None, 16, 16, 512)	0
block5_conv1 (Conv2D)	(None, 16, 16, 512)	2359808
block5_conv2 (Conv2D)	(None, 16, 16, 512)	2359808
block5_conv3 (Conv2D)	(None, 16, 16, 512)	2359808
block5_conv4 (Conv2D)	(None, 16, 16, 512)	2359808
block5_pool (MaxPooling2D)	(None, 8, 8, 512)	0
flatten_1 (Flatten)	(None, 32768)	0
dense_1 (Dense)	(None, 1024)	33555456
dropout_1 (Dropout)	(None, 1024)	0
dense_2 (Dense)	(None, 1024)	1049600
dropout_2 (Dropout)	(None, 1024)	0
dense_3 (Dense)	(None, 7)	7175

Total params: 54,636,615
Trainable params: 54,524,039
Non-trainable params: 112,576

Figure 3. Model architecture for VGG19 based model used in this work

Remarkable progress in machine-based image classification tasks was made due to the availability of large annotated datasets (e.g., ImageNet) and the advances made with

deep learning methods with Convolutional Neural Networks (CNN). However, large annotated datasets in heterogeneous coastal landscapes do not exist. Building a dataset on the scale of ImageNet requires significant efforts. An additional challenge is single class identification owing to the presence of overlapping class traits in the same image. Furthermore, several coastal landscapes, such as beaches, have few identifiable features that define the class as compared with other landscapes such as rocky coasts. Owing to limited annotated datasets, it is difficult to train a neural network from scratch, due to the large number of parameters that architectures like VGG19 have.

In order to overcome limited quantities of labeled data for coastal landscapes, a process called transfer learning can be used that relies on using pre-trained weights for VGG19 that is trained on ImageNet. In transfer learning, low-level features are transferred from pre-trained CNN's on very large datasets like ImageNet to a large CNN model (VGG19) trained on the small dataset without extensive overfitting, which is monitored via a validation dataset. The basic assumption of this process is that the low-level features that the model has learned from ImageNet classification are similar to those of the smaller image database, in this case coastal landscapes.

The transfer learning approach used here is to take a pre-trained network on ImageNet and copy it without the top classification layers to the target network. The target network on top of the transferred layers has two fully connected layers with a rectified linear unit (ReLU) as activation functions and 50% dropout. The fully connected layers, where each neuron is connected to every neuron on a following layer, are part of the neural network classifier based on feature maps extracted by the previous convolutional layers. The ReLU activation function adds nonlinearity to the model, which is required in order to solve anything more complex than a linear fit. The 50% dropout is a common approach to regularizing neural networks, where only 50% of neurons in the fully connected layers are active in each computation, and is used to control overfitting. The remaining layers of the target network are then randomly initialized and trained toward the target task. The choice is made to back propagate errors from the new task into the mid layers of the base (copied) features to fine-tune them to the new task while the very bottom transferred feature layers are left frozen, meaning that they do not change during training on the new task. If the

target dataset is small and the number of parameters is large, fine-tuning may result in overfitting, which is monitored via validation dataset.

The target network is developed using Keras with Tensorflow backend. Amazon Web Services (AWS) Elastic Compute Cloud (EC2) with GPU instances are used for training and inference. The best result with the VGG19 architecture was with five bottom frozen layers and the rest of the layers including classification layers on the top of the network trainable. Models with zero frozen layers to 12 frozen layers were tested to optimize model performance.

From each coastal category class 850 images were used to train the VGG19 to a level of 90% or greater accuracy of successful classification. A further 200 images from each distinct class were used for the validation VGG19 to determine the accuracy of the training phase. There were 90 randomly selected images from each coastal class bin that were hidden from the entire training and validation accuracy processes. These unseen images were the true "test" and yielded unbiased machine results depicting the binned coastal classes.

B. MODEL CONFIDENCE LEVEL

Performance of the classification task is summarized with the use of a confusion matrix (Figure 4), which presents counts of all testing instances based on their actual class and the class predicted by the model. Model confidence level is achieved through the validation process and can be used to confirm the model's accuracy but also as a diagnostic tool to indicate areas where the model performance is less than the desired outcome. Output categories with poor accuracy (defined as a class prediction that is not present in the image) can be addressed in a couple ways. For example, a model output of 33% sandy beach, 33% salt marsh, and 33% dunes, for the validation of 200 pre-classified sandy beach images indicates the model has equal confidence that salt marshes, dunes, and sandy beach are all present in the image. A second example, is a model output of 80% sandy beach, 10% salt marsh, and 10% dunes, for the validation of 200 pre-classified sandy beach images is still not at the desired 90% accuracy, but in this case further training with new sandy beach images might be a tactic to try, which may increase the output accuracy to the desired 90%

instead of dismissing the category completely or merging it with another. Confusion matrices during the testing phase are extremely important tools to show where model deficiencies might be occurring and what methods can be used to correct the problems.

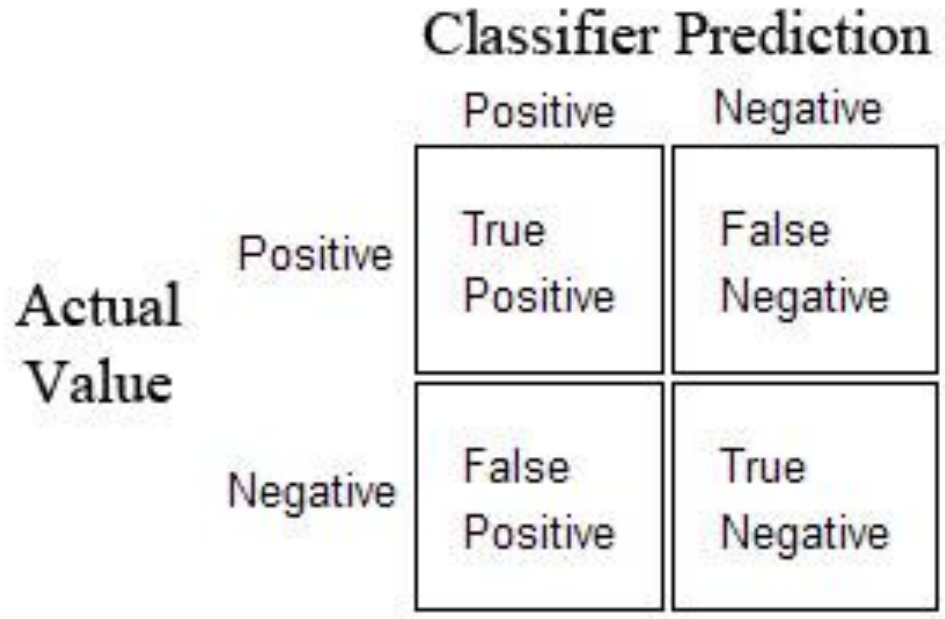

Machine predicted classifier on the horizontal axis and the actual true value for the image on the vertical axis.

Figure 4. Basic schematic of a confusion matrix.
Source: Banda et al. (2013).

Model confidence level relies heavily on training and validation images, with a high degree of homogeneity, these images need to have captured the desired coastal feature, and at the same time minimize features of other coastal categories of interest. Ideally, an image of a rocky coast would be only rocky coast; however, most coastlines exhibit multiple landscapes that represent more than one category. For example, a heterogeneous image may have a forefront of sandy beach and dunes but also have a coastal waterway and or marshes in the background. In this instance, we would have four categories expressed in one image. Images captured from elevation whether from a coastal camera on a building, or hillside to a low slow flying aircraft usually encompass a large dynamic area that is not

homogeneous to any one type of coastal classification category. They may also capture areas of the sky and open water, which may be undesirable for coastline classification purposes.

A tiling technique, better known as image segmentation was developed as a means to combat these issues by breaking an image up into smaller more homogeneous regions (Kuleli et al. 2011) to be classified. Image segmentation is a form of supervised training that consists of learning how to map input data to a known data set (Chollett 2018).

The use of image segmentation was applied to a large morphodynamic region in California's Central Coast, specifically Carmel River State Beach (CRSB). There are five large mosaics of CRSB represented over a six-month period from December 2017 through May 2018. During this time, Carmel River was opened and closed to the Pacific Ocean, which was captured in the different mosaics. Dynamic differences in the lagoon water level can easily be depicted by the eye and exposure of coastal rock formations from sand erosion and many other easily discernable macro feature changes that are identifiable. By applying image segmentation, breaking CRSB into smaller pieces and using the machine learning coastal image classification model, the goal is to identify areas of significant beach change (e.g., Carmel River breached vs non breached and lagoon full vs lagoon drained).

C. AERIAL DATA COLLECTION AND DATA BASES

The coastal imagery used in this study was primarily collected from 2002 through 2018, by a low slow-flying fixed wing aircraft and remote piloted UASs using digital cameras along the United States coastlines, including West, East, and Gulf Coasts, representing various types of coastal landscape categories. The majority of the imagery was taken at camera angles that captures 50% or greater the coastal features desired but also contains portions of open water and the sky. Photographic images of the East, Southeast, and West coasts of the United States were all examined; both rural and developed areas are present in most of the respective areas. The imagery library datasets were composed of three sources: West Coast (California Coastal Records Project, https://www. californiacoastline.org/), Gulf Coast (Mara Orescanin, NPS), and East Coast (NOAA, Coastal Imagery Viewer).

The individual images in this library represent a heterogeneous mix with major influencing factors including, their variability attributed to the temporal scale of when the images were taken, different camera types, differences in flight level, sun angle, intensity, glint change, and camera angle variation.

D. CLASSIFICATION OF COASTAL IMAGERY

Eight original different categories were chosen to bin this data based off of sufficient representation from the collected aerial imagery and expected landscapes observed at the Carmel River system. The bins were broken down into the following descriptive coastal landscape classes: coastal cliff, coastal rocky, coastal waterway, dunes, man-made structures, salt marshes, sandy beaches, and tidal flats based off of NOAA classification for coastal landforms (NOAA 2013). Each bin contains 1100 class specific images. All heterogeneous images were manually examined and classified based on the predominant class-defining feature. For example, a large sandy recreational beach with some lesser areas of salt marsh inland would be classified into the sandy beach category. The idea behind this is that if the dataset is expansive enough (shows diverse representation of each class), the neural network will be able to identify the areas of the image that correspond to each class, regardless of the presence of other classes in each image. Borderline images and images with multiple features represented, such as a 50% (+/- 10%) coastal waterway and salt marsh were discarded. It was thought that two or more dominant features would result in confusing the model during the training process, and cause increased levels of both type I (false positive) and type II (false negative) error that would lower the accuracy of successful classification.

E. CARMEL RIVER STATE BEACH TILING AND CLASSIFICATION

There were five mosaics of CRSB composed using data collected on December 7, 2017, January 11, 2018, January 23, 2018, February 28, 2018, and May 17, 2018. The data was collected by a Da Jiang Innovations (DJI) Phantom III Advanced quadcopter equipped with a twelve-megapixel camera having a ½.3” sensor and f/2.8 prime lens. The UAS was flown at ~60m elevation and at a speed of 5 m/s, the camera set to 10 degrees off nadir and

fast mode triggering was enabled. The images collected from each date were stitched together using Agisoft Photoscan version 1.4 software.

The large mosaics of CRSB represent a wide range of coastal features, and it would be difficult to assign any one class to the large image because of its heterogeneity. In order to make images of similar scale to the training dataset and easier to classify, image tiling was applied to the larger mosaic, breaking it into smaller more manageable pieces. The large mosaic was broken down using a script written in MathWorks MATLAB software into 2 by 2 and 3 by 3 rows and columns. Each tile was equal with respect to the amount of area it represented when compared to another tile of the same dimension. The tiled images were labeled using an alphanumeric scheme (Figure 5), numbers represented the columns and letters represent the rows. Each tiled image was individually examined, and classified into one of the nine previously described bins based solely on the user identifying the most dominate feature. In some instances, lesser features were noted but a label was not applied to the image with regard to these notes.

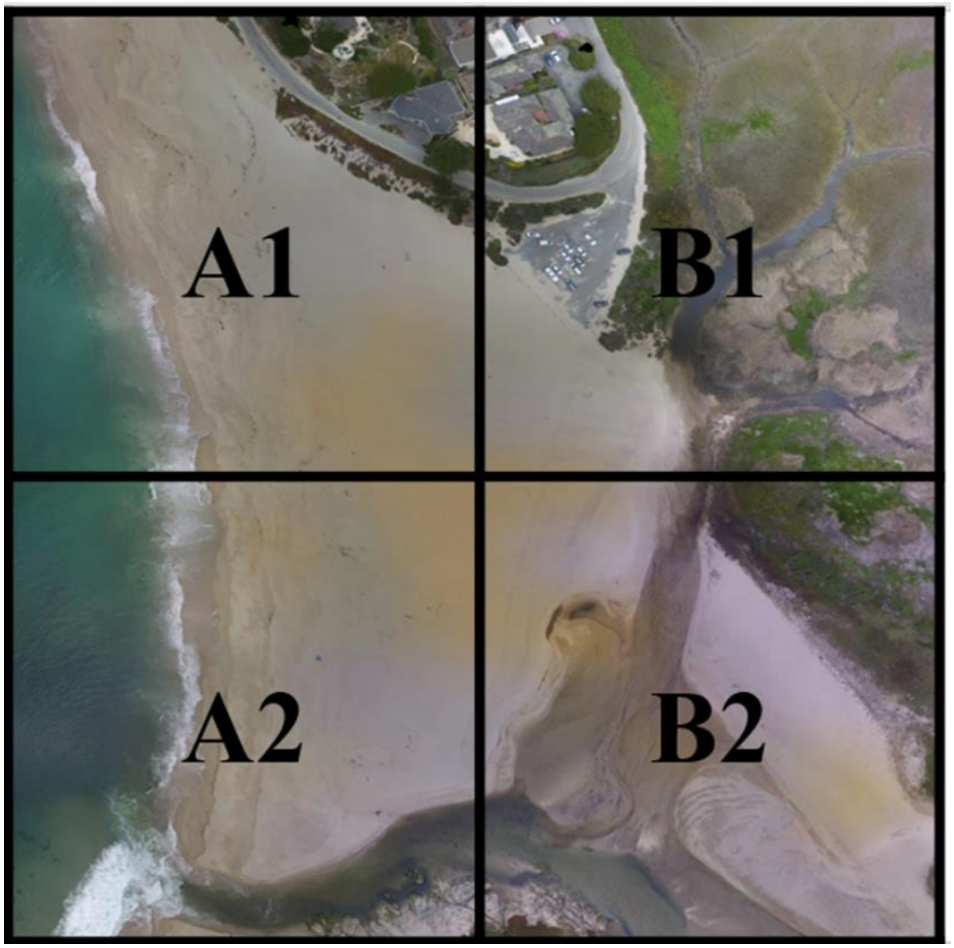

Rows are numeric in descending order starting from 1. Columns are letters starting at A and increasing from left to right.

Figure 5. Two-by-two image tiling naming scheme, depicting CRSB on May 17, 2018.

F. PROCESSING OF MOSAICS TILED IMAGES

Both the 2x2 and 3x3 tiled images sets for the CRSB mosaics were processed identically. The Python programming language and VGG19 model architecture was used to classify the tiles into one of eight coastal categories. The VGG19 assigns values to each of the eight categories that it was trained on, even though each category had some value, the highest assigned value wins and the tile is labeled to reflect that.

Once all mosaics were tiled and classified into one coastal category by VGG19 and the user, these results were compared over the five different dates, and the labeling was

assessed to determine how the areas prone and known to seasonal change were classified by VGG19 and the user. By using 2x2 and 3x3 tiling strategies, it was thought that the 3x3 tiling would provide better homogeneity to specific coastal features when compared to 2x2 tiling, and therefore be better able to identify through change detection the different morphodynamic areas of CRSB.

MathWorks MATLAB software was used to display the tiled mosaics and associated output graphs. This method provided an effective means to analyze the tile with its respective machine learning output bar graph, allowing the user to easily identify what each tile was labeled.

IV. RESULTS

A. TESTING OF THE COASTAL IMAGERY IN THE DEEP LEARNING NEURAL NETWORK

Upon completion on the neural network training and validation, the test images, comprised of 90 randomly selected images per class were used to assess model accuracy. In addition, new images of Carmel River State Beach, completely outside the image database, were used to further test the neural network and to develop change detection algorithms. The accuracy of the trained model was assessed using the remaining 10% of images from the labeled database that were not used in the training and validation of the model parameters. Label output by the model was compared to the hand-classified label. The result of this test is a confusion matrix (Figure 6), where the blue diagonal squares show the accuracy of the model using the testing images sets for each coastal class. Perfect accuracy would be a diagonal matrix with all 1.0 values on the diagonal. This matrix is normalized by the number of images in each class to denote a percent accuracy, but all categories had 90 images to test. Sand dunes was the most accurate and salt marshes the least accurate at 100% and 88% respectively. A closer examination shows salt marshes and tidal flats classes were being mislabeled at a rate of 5-6%, which was higher than the other classes.

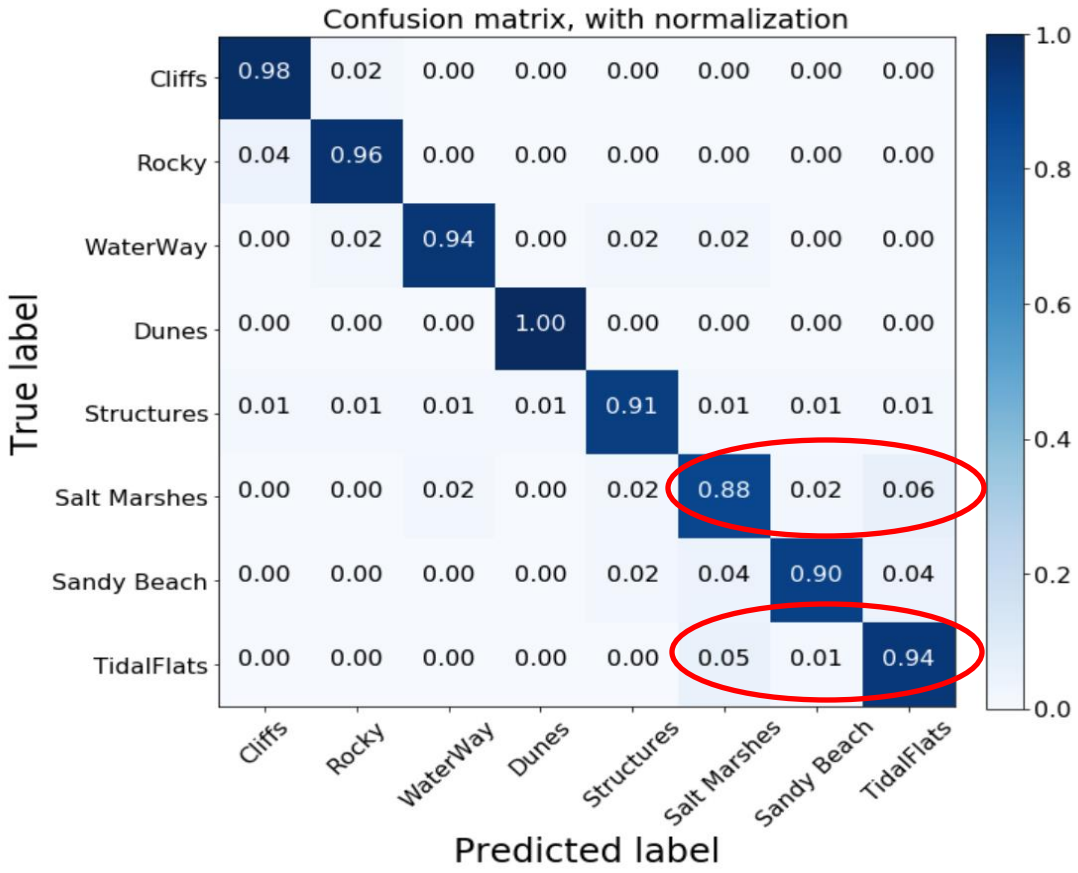

Diagonal blue boxes represent percent accuracy with respect to image class labeling. 1.00 is 100% and other decimal values represent percentage accuracy in similar fashion.

Figure 6. Confusion matrix constructed from test image results

One way to determine where a certain class exists within an image is to use a class activation map, or heat map. This algorithm highlights the percentage that regions within an image belong to the class in question. The labeling of the classes (Figure 7, left) chosen through deep learning was confirmed using a heat map program (Figure 7, right) designed to make visually recognizable where the neural network identified a feature or gradient it recognized as attributable to the labels it chose.

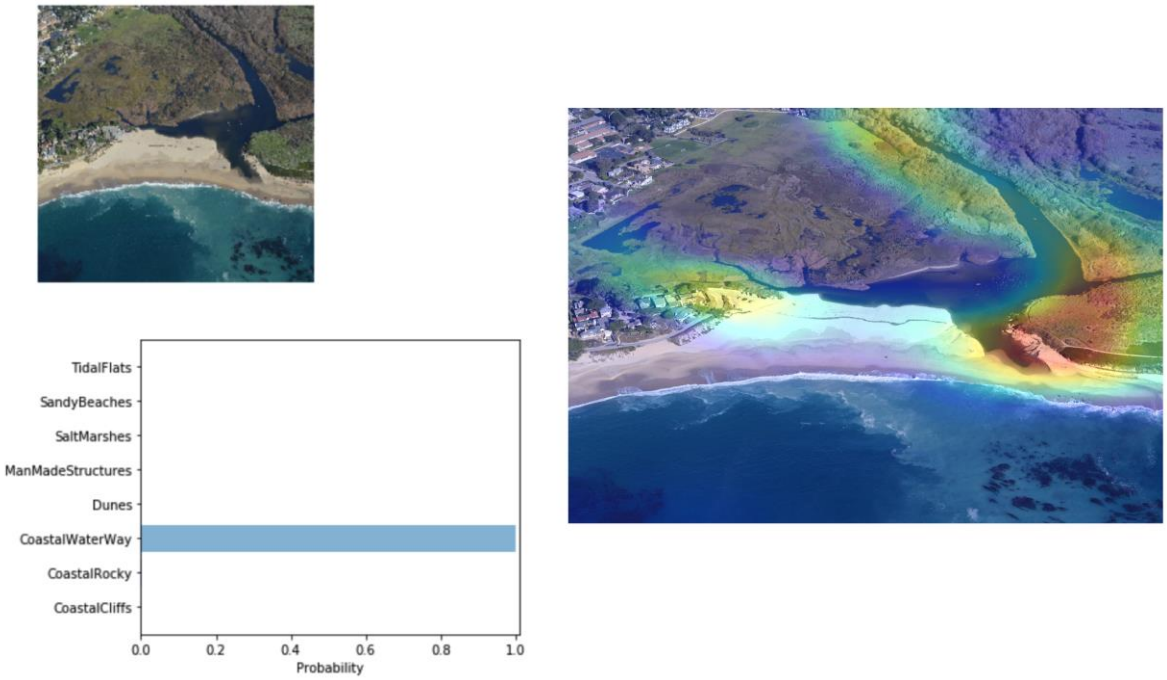

Left side deep learning labeling and right side heat map verification. Warmer colors on heat map indicate areas where features and gradients were identified and associated with the label assigned.

Figure 7. December 20, 2016, CRSB, oblique single camera image

B. CHANGE DETECTION AT CARMEL RIVER STATE BEACH

The five different mosaics (Figure 8) of CRSB capture the typical seasonal variability of coastal landscapes found at this ephemeral river. In the six and a half month period spanning from early December 2017 through mid-May 2018 there is an increase in water level forming a lagoon owing to increased precipitation. When the water height is level with the surrounding barrier beach, there is a breach into the Pacific Ocean emptying the lagoon and exposing coastal rocks, tidal flats, and creating a new coastal waterway between the lagoon and the Ocean seen in the January 11 image. The January 23 mosaic the lagoon is drained and the breach is closed, and within roughly one-month time, the lagoon begins refilling and on May 17. There is another breach that again drains the lagoon completely.

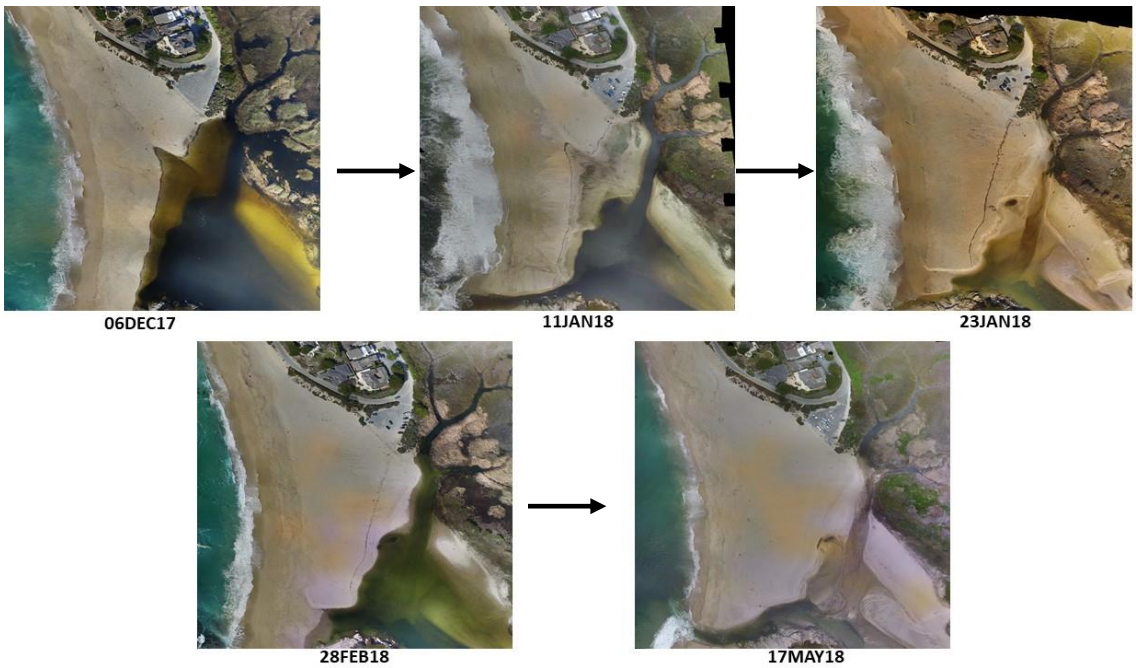

Mosaics from early December 2017 through mid-May 2018. Mosaics progress in time from left to right and top to bottom.

Figure 8. Five CRSB mosaics

Mosaics of CRSB were tiled into 2x2 matrices to break up the large area for two reasons. First, to divide equally CRSB into 4 tiles results in smaller sections with a more representative area and features of the same scale when compared to the images used to train the neural network. Second, it was thought that this approach would make the images more homogenous and resulting in better labeling results from deep learning. All 5 mosaics had this approach. Results for January 11 and 23, 2018, and February 28, 2018, are in Appendix A.

1. December 6, 2017, Mosaic

In the December 6 mosaic (Figure 9), the lagoon is full, the coastal water way is very pronounced, and there is no river breach into the Pacific Ocean. Column A shows the ocean side of CRSB and deep learning results indicates strong outputs of coastal water way and salt marsh for tiles A1 and A2 respectively. These results were not the expected results; the main eye catching feature is a beach in both tiles. However, the deep learning method picks up on gradients and features that caused these tiles to be labeled differently than one

would expect. The B column is the inland portion of the mosaic and is tiled in similar fashion as the A column. The B1 tile had a dominant label of coastal waterway, which is a major feature that is dead center in the tile. The B2 column showed mixed result of coastal cliffs, rocky coast, sandy beaches and tidal flats. This result with no dominate label for the image indicates that the deep learning process has seen features and gradients of the four classes in almost equal proportions and labeled them accordingly.

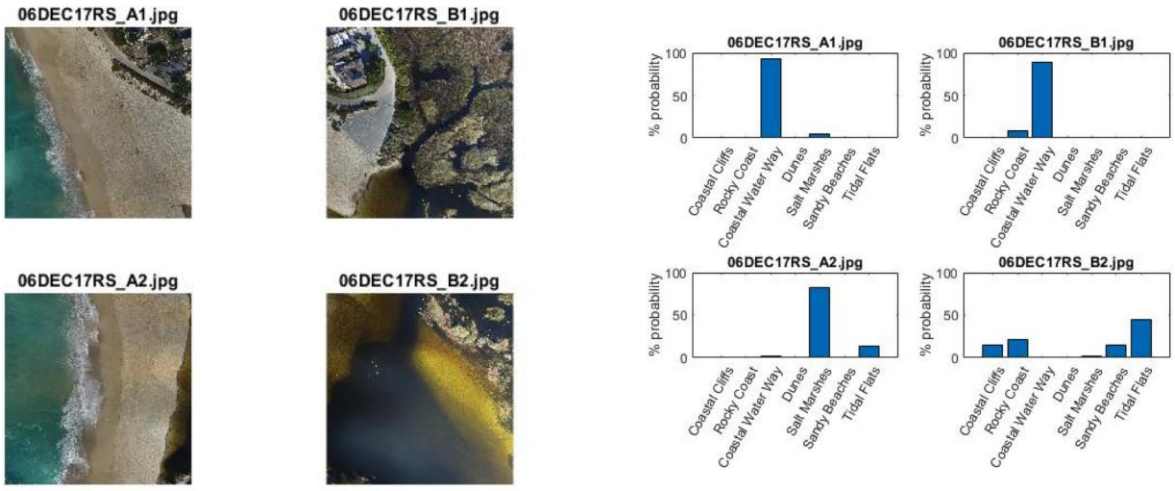

Mosaic tiled into 2x2 matrix (left) and graphical representation (right) of deep learning outputs with respect to each tile.

Figure 9. December 6, 2017, CRSB mosaic

2. May 17, 2018, Mosaic

May 17 mosaic (Figure 10) is strikingly different from the December 6 mosaic. However, column A had, in similar fashion to December 6, strong indications of the salt marsh class for A1 and of the tidal flats class for A2. The model picked up on features and gradients in a similar fashion to December 6 that resulted in mislabeling. The predicted classes for these two images were sandy beach and sandy beach or coastal waterway respectively. The landward portion of this image is drastically different from December 6, owing to the breach that caused drainage in the lagoon and reduced the extent of coastal

waterway. Column B had class labels matching the predicted labels of salt marsh for B1 and tidal flats for B2

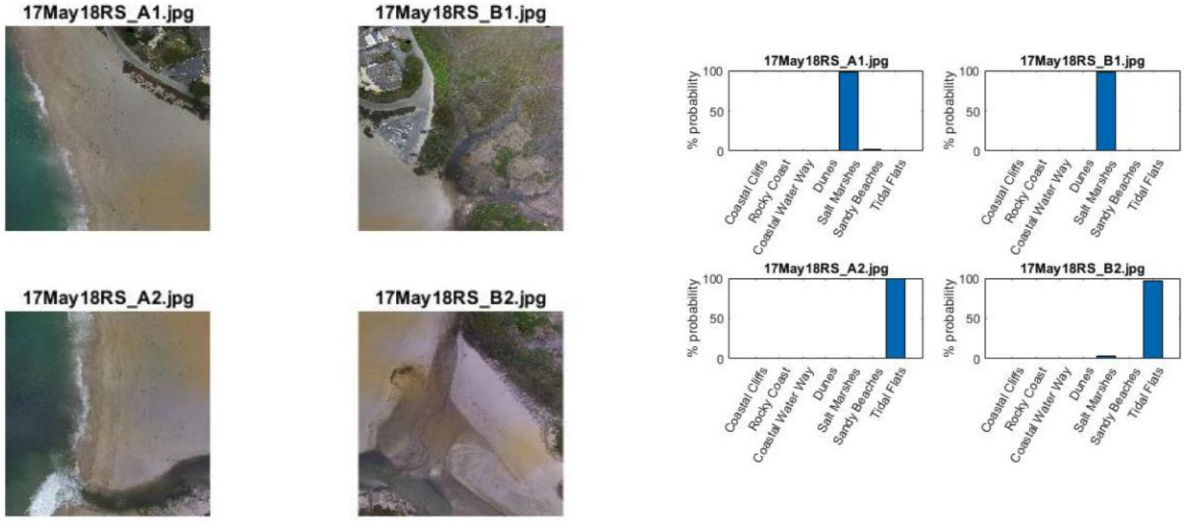

Mosaic tiled into 2x2 matrix (left) and graphical representation (right) of deep learning outputs with respect to each tile.

Figure 10. May 17, 2018, CRSB mosaic

C. ANALYSIS OF TILED CRSB MOSAICS IN 3X3 MATRICES

All 5 CRSB mosaics were also tiled into 3x3 matrices in a similar fashion to the 2x2 tiling scheme in order to assess whether the model performs better with a smaller field of view. The 3x3-matrix scheme was thought that the increased homogeneity and slightly smaller images would produce more definitive labeling to match predicted labeling through the deep learning process. Results for January 11 and 23, 2018, and February 28, 2018, are in Appendix B.

1. December 6, 2017, Mosaic

A visual inspection of the 3x3 matrix for December 6, 2017, (Figure 11) immediately reveals a more homogenous landscape for each tile. Column A depicts really well three images of a sandy beach with visually what appears to be very little influence from then other 7 classes. Column B yielded similar results sandy beach transitioning into

a salt marsh in images B1-B3, respectively. Column C, which represents the most inland portion of the image, visually shows the tiling process's ability increase homogeneity. It is easy to detect a change from coastal waterway to a salt marsh and tidal flat landscape.

The deep learning results had some significant differences than the expected outcome using qualitative inspection of the images. Column A had sandy beach representation in all three tiles; however, this was not the dominant feature that would have matched the prediction. Column B did much better with the exception of B1, which was predicted to be sandy beach. However, instead B1 showed equal or higher values of representation of coastal cliff and rocky coast, as well as, a significant measure of coastal waterway when compared to sandy beach result. Column C had surprisingly difficulty identifying the coastal waterway in C1. The C2 image also had mixed results showing good representation of tidal flats in conjunction with equal or greater values coastal cliff, rocky coast, and sandy beach.

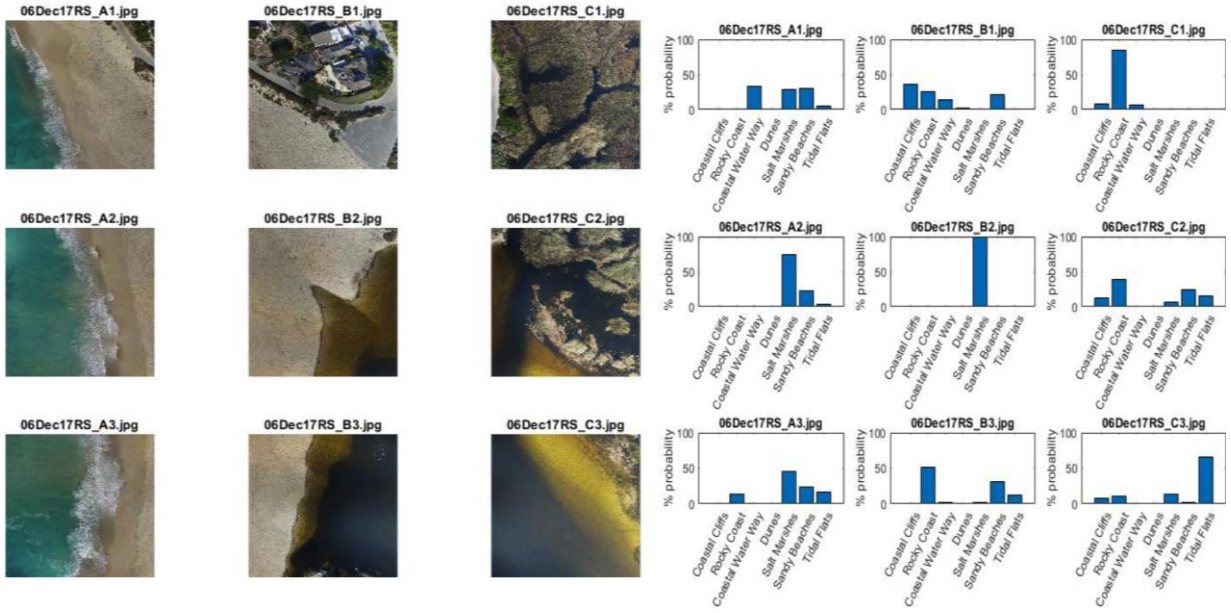

Mosaic tiled into 3x3 matrix (left) and graphical representation (right) of deep learning outputs with respect to each tile.

Figure 11. December 6, 2017, CRSB mosaic

2. May 17, 2018, Mosaic

The May 17, 2018, tiling process (Figure 12) yielded results visually similar to December 6, 2017, increased homogeneity while still capturing one or more of the targeted classes. Column A differs from the December 6, 2017, most noticeably in tile A3 where the Carmel River has breached into the Pacific Ocean. In column B, the striking difference is the salt marsh has drained resulting in what appears to be sandy beach and tidal flat with exposed rock for tiles B2 and B3, respectively. Column C, in the same fashion as Column B, shows the results of the drained salt marsh. The coastal waterway in tile C1 has reduced in size and appears to be more salt marsh like. The C2 tile has also been significantly drained from the breach with little water left visually indicting a salt marsh and tidal flat appearance. C3 has strong visual indications of tidal flats with possibly some sandy beach.

Deep learning results for column A showed a strong deviation to the salt marsh and tidal flat classes with little or sandy beach and coastal waterway representation from A1-A3 tiles. The B column with the exception of B3 showed different results then predicted, B1 and B2 were both predicted to be sandy beach. However, salt marsh and tidal flats were the labels assigned through deep learning. B3 was label tidal flat which is what was predicted but it did miss the exposed rocks at the bottom of the tile. The C column was successful for all three tiles; C1 and C2 were labeled as salt marsh as the dominant class with negligible representation from any other class. C3 was very confident with tidal flats with no other classes having significance.

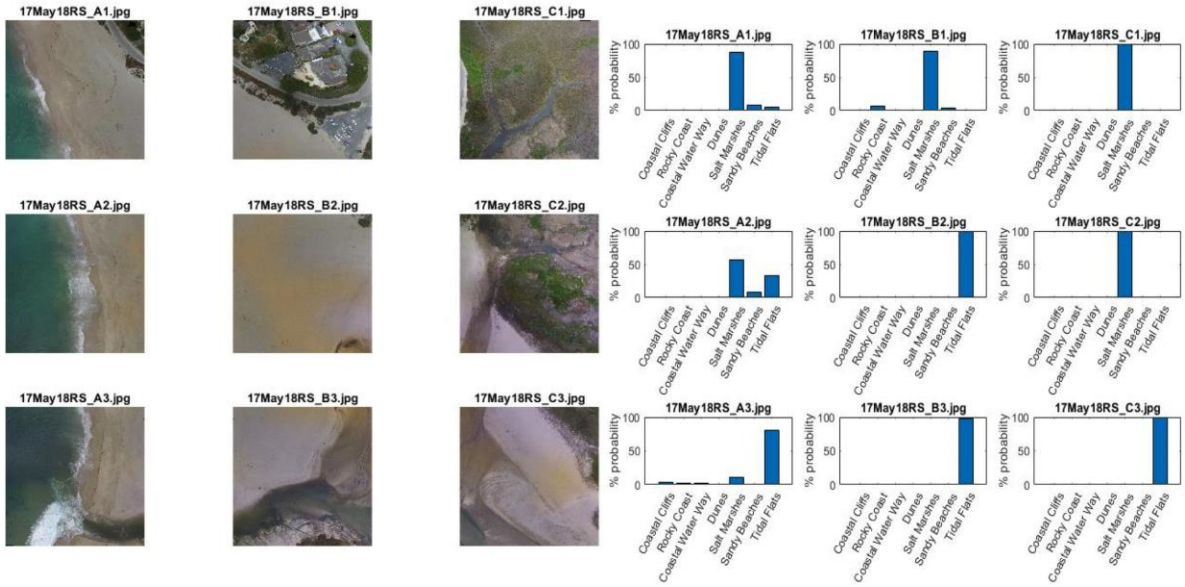

Mosaic tiled into 3x3 matrix (left) and graphical representation (right) of deep learning outputs with respect to each tile.

Figure 12. May 17, 2018, CRSB mosaic

D. MOSAIC STITCHING ANALYSIS USING HEATMAP FOCUSING

Further analysis was needed for the 2x2 matrices in an effort to locate the source of the gross errors in labeling when compared to the predicted labels. Tile A1 was selected from each mosaic for examination using a heat map. Tile A1 is a good representation of a homogenous sandy beach at both December and May mosaics and serves as a control between the two dates. Heat map gives a visual focal point to where the deep learning process has identified certain features and gradients that belong to a certain class.

A closer examination of the tile A1 using a heat map for each mosaic revealed hotspots in areas that were not consistent with the training labeled data set for the respective category. Figure 13 is the December 6 A1 tile and shows this inconsistency where hotspots for salt marsh are visually located over the surf zone and sandy beach.

Demonstrating using a heat map (right) to identify marsh areas through deep learning. Warmer colors on heat map indicate areas where features and gradients were identified and associated with the label assigned.

Figure 13. December 6, 2017, tile A1 from 2x2 matrix

Focusing in on the salt marsh in the surf zone hotspot (Figure 14), there are stitching issues evident that are not seen from a farther out view. This smearing and gradient distortion from the stitching process in areas where there was significant surface motion were observed consistently in the water and surface zone regions in tile A1.The creation of these artificial gradients biased model prediction toward other non-homogenous classes, as a result incorrect labels were assigned.

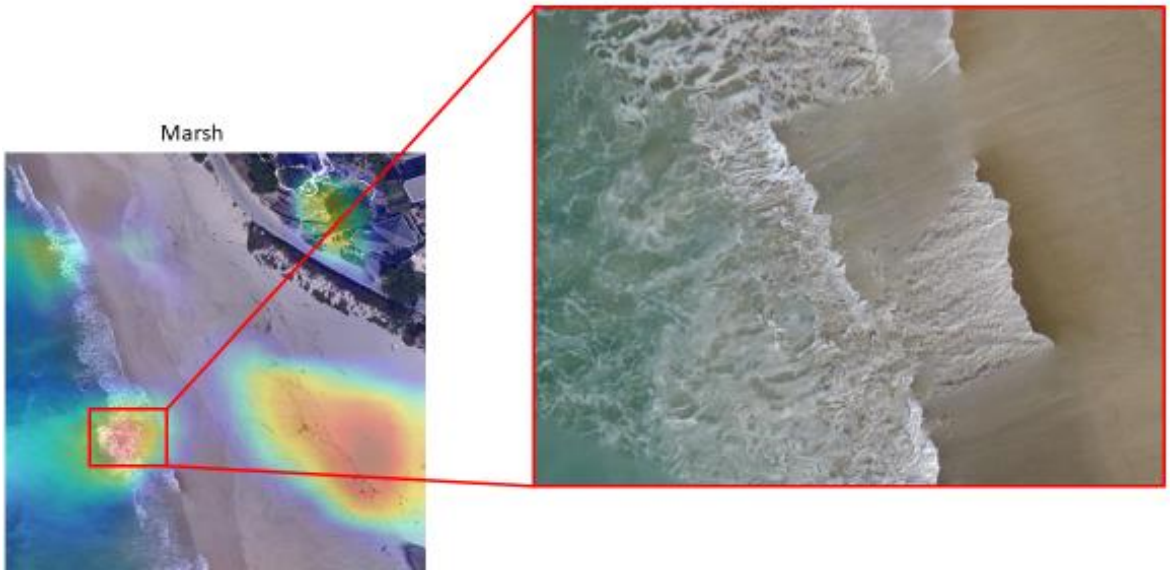

Using a heat map (left) and zoomed in hot spot area (right) highlighting image stitching and gradient concerns.

Figure 14. December 6, 2017, tile A1

May 17 A1 tile showed a similar miss labeling of salt marsh (Figure 15). A salt marsh hotspot was located off the beach in this case and in a residential area. Using the same approach as December 6, the hotspot marsh area was focused in on (Figure 16) and again noticeable stitching issues were apparent. The wind was blowing on shore during the capture of the images and a similar effect to December 6 A1 tile in the surf zone was see inland in the May 17 A1 tile.

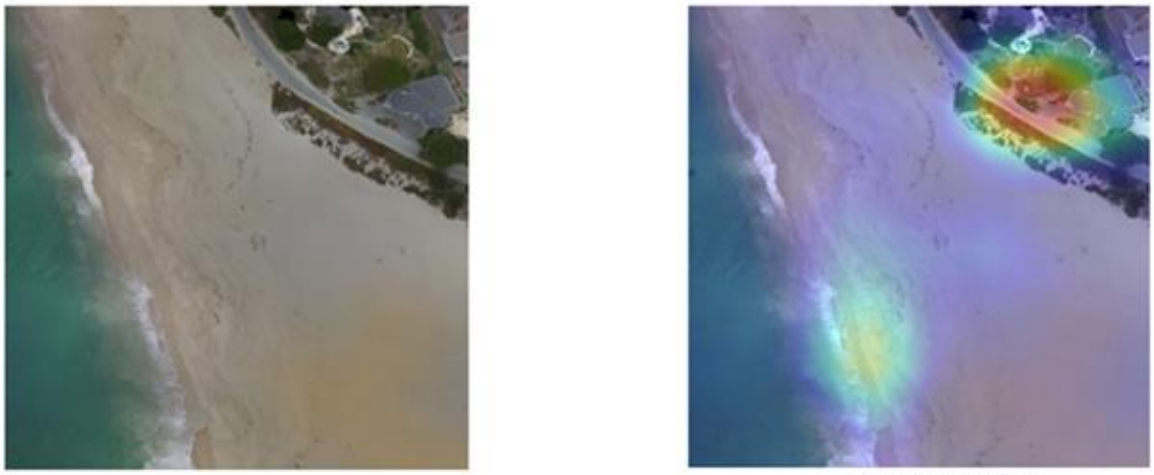

Demonstrating using a heat map (right) to identify marsh areas through deep learning. Warmer colors on heat map indicate areas where features and gradients were identified and associated with the label assigned.

Figure 15. May 17, 2018, tile A1 from 2x2 matrix

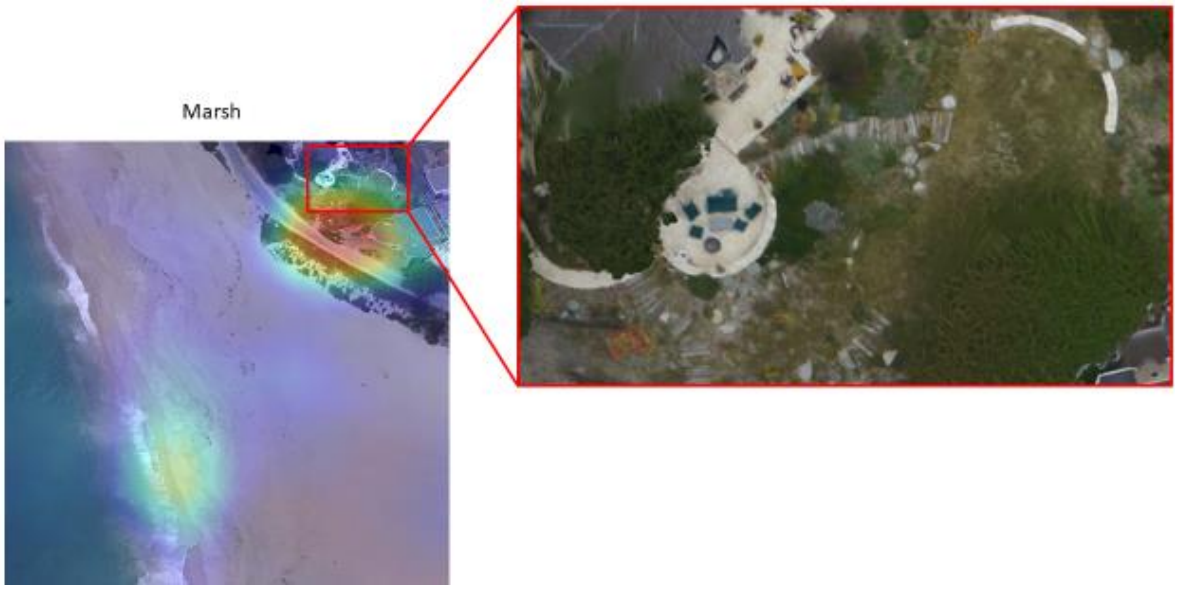

Use of a heat map (left) and zoomed in hot spot area (right) highlighting image stitching and gradient concerns.

Figure 16. May 17, 2018, tile A1

E. OBLIQUE SINGLE IMAGE ANALYSIS OF CRSB CHANGE DETECTION

CRSB was also analyzed at an oblique angle similar to images used to train and test the VGG19 model. Two significantly distinct images were used to test the mode for change detection. Figure 17 is a comparison of non-breached Carmel River (December 20, 2016) and breached Carmel River (January 23, 2017). Coastal water way was properly and accurately labeled in both images and confirmed using heat maps. The breached image shows a new hot spot correctly placed and labeled for coastal waterway when compared with the non-breached image.

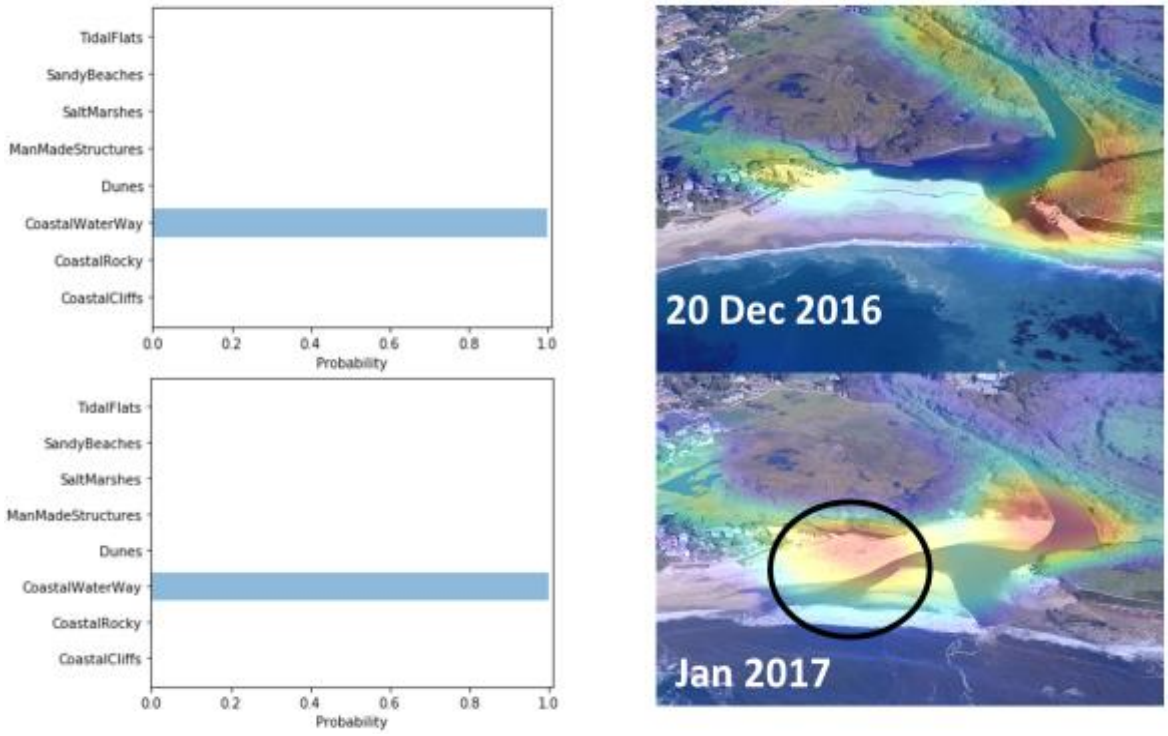

Depiction of oblique single camera image. Left side deep learning labeling and right side heat map verification. Warmer colors on heat map indicate areas where features and gradients were identified and associated with the label assigned.

Figure 17. December 20, 2016, (top) and January 23, 2017, (bottom) CRSB

THIS PAGE INTENTIONALLY LEFT BLANK

V. DISCUSSION

The results indicate that using deep neural networks, specifically through transfer learning, is an effective method to classify heterogeneous coastal landscapes without the need for semantic segmentation. Despite the heterogeneity of the training dataset and its relative small size compared to ImageNet (10000 images vs. over 1 million images), there is enough difference between each coastal class implying correct identification is possible. This method shows potential for automatic classification of coastal landscapes, which can help increase efficiency for identifying areas of change.

It was noticed that images where the dominant feature was sandy beach or tidal flats were difficult to correctly identify in the unseen test images, especially at Carmel River State Beach. One possible explanation for this is the lack of gradients within these landscapes compared to those within rocky coastlines, marshes, and coastal waterways. Therefore, it is expected that these areas will be under-identified, which highlights a need to weight these classes differently for future training efforts.

The coastal change detection algorithm using deep learning detection can be improved upon in a number of ways. First, given the inherent heterogeneity of coastal landscapes, it would be advantageous to use a multi-label approach to increase the sample size of each class. This could, in turn, allow variable image sizes to be classified by the model. Second, in this study, large images (tifs) compiled through Structure from Motion were broken down into 2x2 and 3x3 matrices in an effort to increase homogeneity within the sub-images and create sections of the larger image that were comparable in size to the imagery used to train the deep neural network. This method was determined to be inadequate owing to artifacts from stitching the UAS imagery together. Instead, it would be worthwhile to attempt this method on larger scale images from satellites. Future work could include a finer tiling scheme to target change over smaller areas. Third, it would be advantageous to add more classes of water, such as surfzone, as this is a ubiquitous feature in coastal imagery. In addition, adding classes that include human infrastructure, such as roads, buildings, and boats, would be useful so the model does not classify these areas incorrectly. This micro level (< 1km areas) approach is what is needed for small-scale

tactical military operations and areas where there a rapidly changing environment. The ability to capture large and small-scale changes provides commanders with essential information for the planning stage.

This study specifically focuses on low altitude photographic imagery. The advancements of satellite technology adds to the already large database of imagery. Optical satellites have limitations especially with cloud coverage; however, synthetic aperture Radar satellites (SAR) do not need the Sun to function and are capable in all weather conditions (Costa 2004). The SAR satellite capabilities provides new avenues to take advantage of transfer learning and deep learning techniques discussed in this paper.

This study focuses heavily on the visible light range and optical photography images. The use of other media (infrared) needs to be explored to take further advantage of deep learning. Different vegetation species have their own their own unique infrared spectral features, specifically reflectance and emission, which can be used to classify areas of vegetation according to their spectral characteristics (Xie et al. 2008). The ability to accurately map and categorize vegetation types is important, the growth, decline, and location of species is important for forestry management and location of animal species that are particular to a certain type of vegetation.

The results of this study are driven by proper identification of gradients and features used to flag regions specific to the unique classes. The output for the labeling is verifiable using the heat map. A different approach maybe to use the feature and gradient recognition to label areas for rejection. If this process can be coupled with a multiple reading of the same image at different levels, perhaps a more fined tuned process could be developed with multiple reads of the same image focusing on specific areas selected by the user.

VI. CONCLUSION

It was possible to use heterogeneous coastal landscapes to train a deep neural network through transfer learning and training from scratch with a high degree of accuracy (>90% correct identification) without the need for image semantic segmentation. Overall, 95% accuracy with test images was achieved.

The use of high-resolution UAS imagery of the same coastal site over time coupled with a trained deep neural network will be able to accurately and effectively highlight areas that varies seasonally. The CSRB study site is dynamic and overhead stitched mosaics were effective in labelling and detecting change in the landward part to the mosaic. The mislabeling problems for the ocean side of the mosaics were located using heat mapping, and upon further inspection of the flagged areas, there was noticeable image stitching seams. The seams created false gradients and features not attributable to the actual landscape. These imaging artifacts caused a gross mislabeling of both tiles in the A column for both mosaics.

CRSB mosaics were all comprised of overhead images with little or no offset from nadir. The images used to train, validate, and test the deep learning neural network were captured from oblique angles. This drastic difference in view point and lack of training with overhead images in conjunction with image stitching problems is attributable to labelling errors. In an effort to increase accuracy, much larger datasets will be needed to encompass the different types of coastal landscape on the continental and regional scales. Data set increase coupled with a multi-angle approach for image capture should enhance the deep learning network by giving different visual perspectives and allowing for gradients and features to be extracted from each class.

THIS PAGE INTENTIONALLY LEFT BLANK

APPENDIX A. ADDITIONAL 2X2 MOSAIC MATRICES

A. JANUARY 11, 2018, MOSAIC

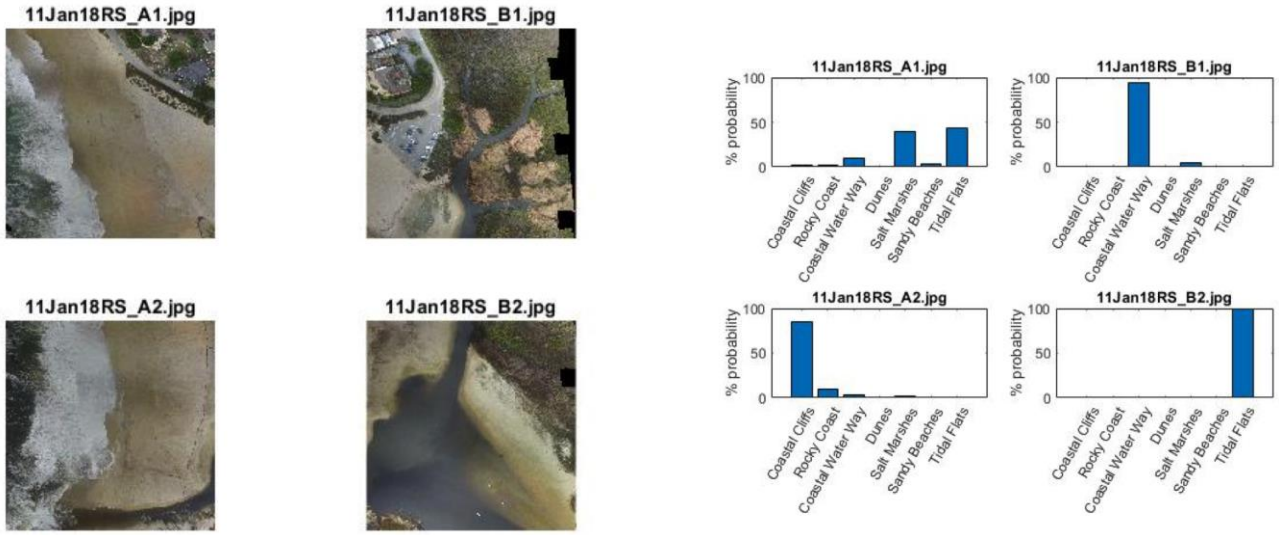

Mosaic tiled into 2x2 matrix (left) and graphical representation (right) of deep learning outputs with respect to each tile. A1 = sandy beach, A2 = sandy beach and rocky coast, B1 = coastal waterway and marsh and B2 = coastal waterway and sandy beach.

Figure 18. January 11, 2018, CRSB mosaic

B. JANUARY 23, 2018, MOSAIC

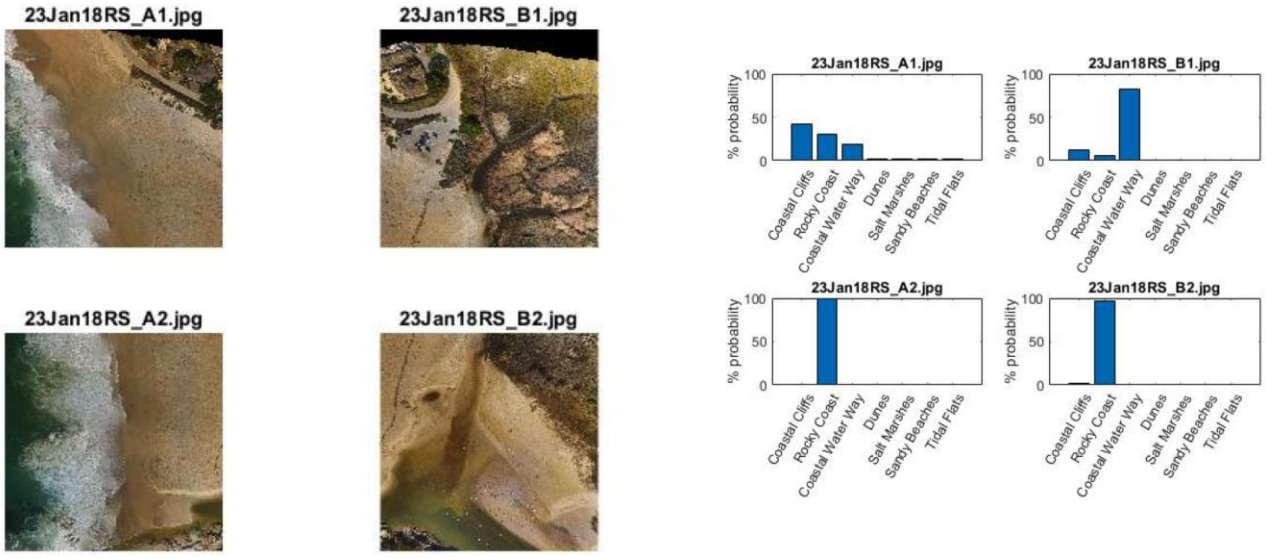

Mosaic tiled into 2x2 matrix (left) and graphical representation (right) of deep learning outputs with respect to each tile. A1 = sandy beach, A2 = sandy beach and coastal rocky, B1 = coastal waterway and marsh, and B2 = tidal flat and coastal rocky.

Figure 19. January 23, 2018, CRSB mosaic

C. FEBRUARY 28, 2018, MOSAIC

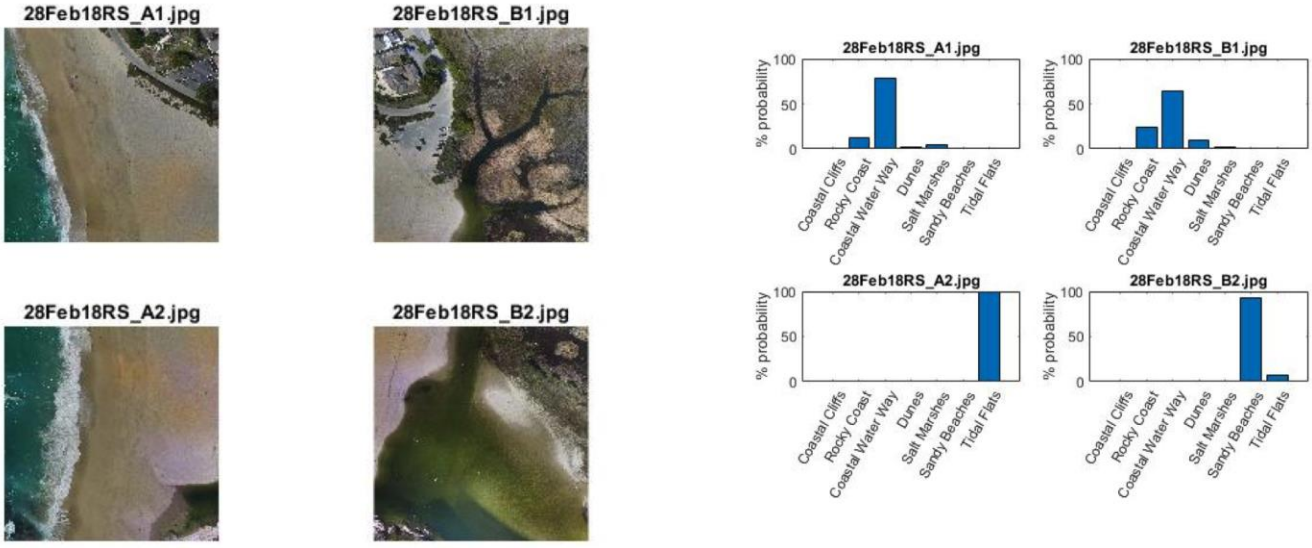

Mosaic tiled into 2x2 matrix (left) and graphical representation (right) of deep learning outputs with respect to each tile. A1 = sandy beach, A2 = sandy beach, B1 = coastal waterway, and B2 = marsh.

Figure 20. February 28, 2018, CRSB mosaic

THIS PAGE INTENTIONALLY LEFT BLANK

APPENDIX B. ADDITIONAL 3X3 MOSAIC MATRICES

A. JANUARY 11, 2018, MOSAIC

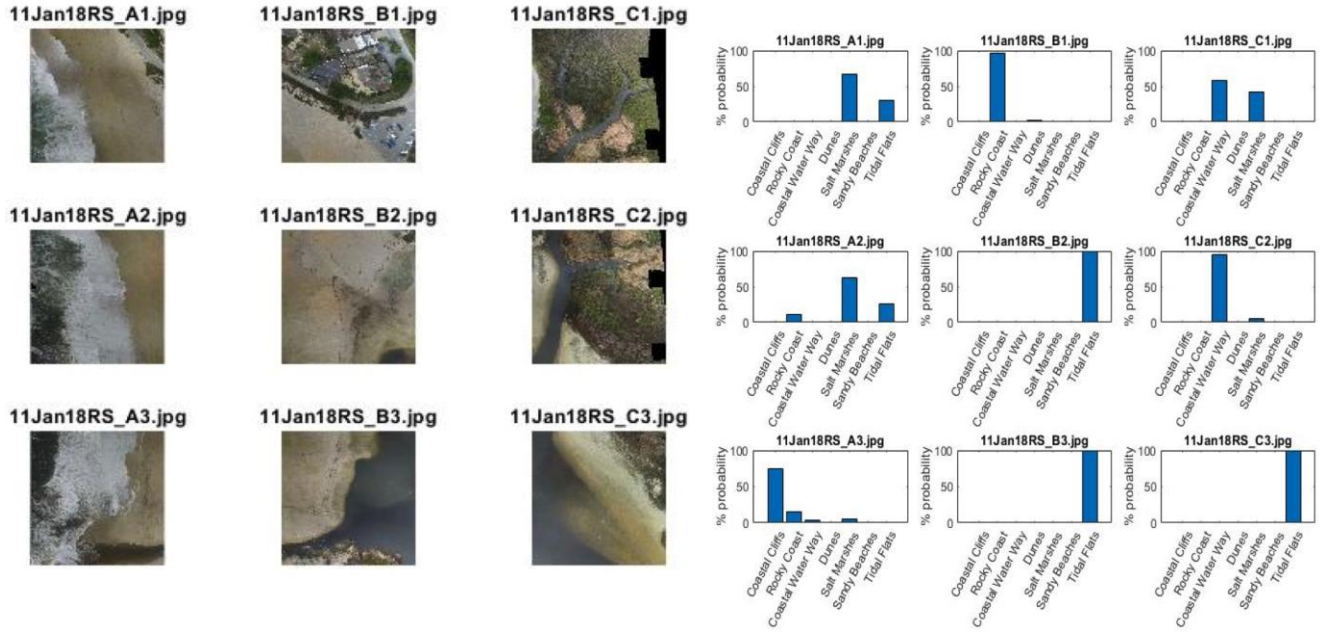

Mosaic tiled into 3x3 matrix (left) and graphical representation (right) of deep learning outputs with respect to each tile. A1 = sandy beach, A2 = sandy beach, A3 = sandy beach and coastal waterway, B1 = man made, B2 = tidal flat, B3 = rocky coast, C1 = coastal waterway, C2 = coastal waterway, and C3 = tidal flat and sandy beach.

Figure 21. January 11, 2018, CRSB mosaic

B. JANUARY 23, 2018, MOSAIC

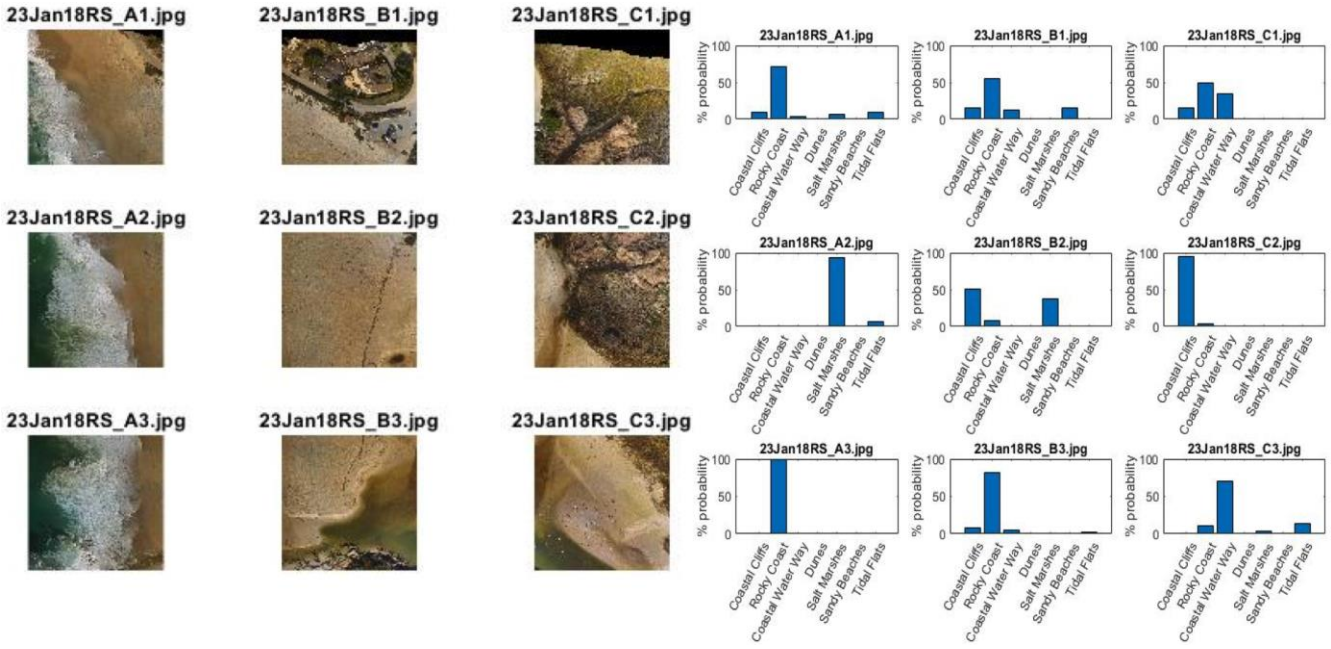

Mosaic tiled into 3x3 matrix (left) and graphical representation (right) of deep learning outputs with respect to each tile. A1 = sandy beach, A2 = sandy beach, A3 = sandy beach, B1 = man made, B2 = tidal flat, B3 = rocky coast and tidal flat, C1 = coastal waterway, C2 = tidal flat and marsh, and C3 = tidal flat and sandy beach.

Figure 22. January 23, 2018, CRSB mosaic

C. FEBRUARY 28, 2018, MOSAIC

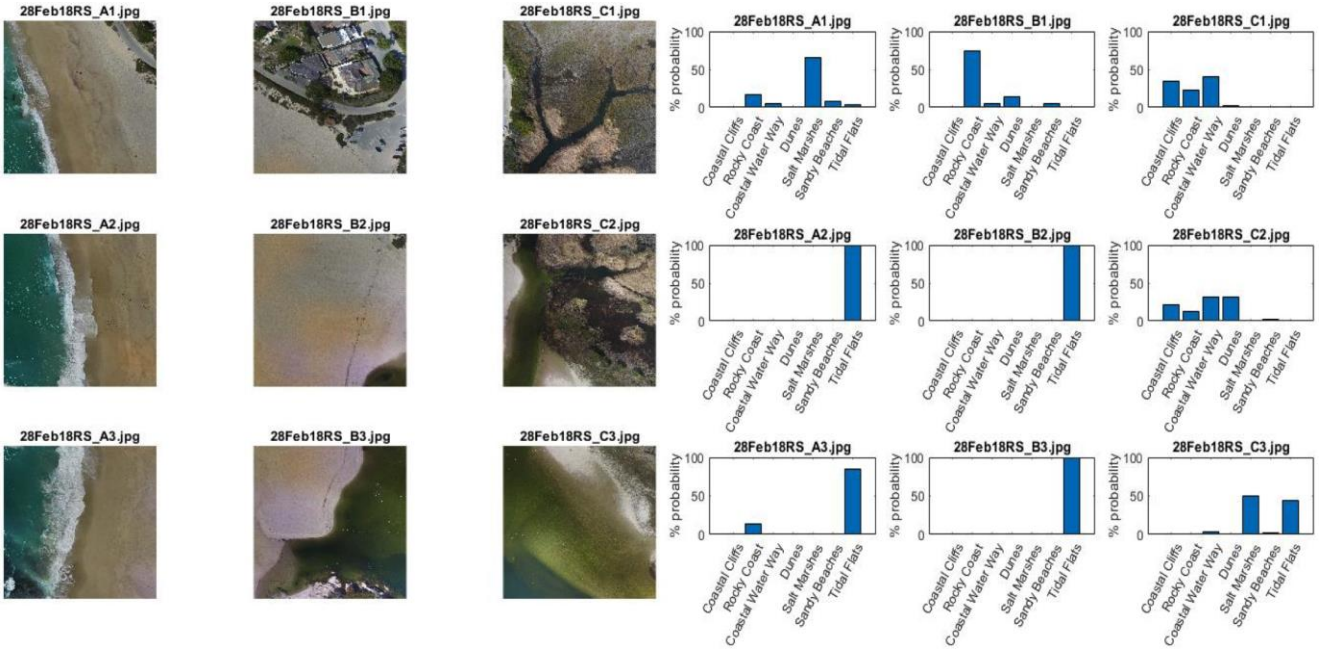

Mosaic tiled into 3x3 matrix (left) and graphical representation (right) of deep learning outputs with respect to each tile. A1 = sandy beach, A2 = sandy beach, A3 = sandy beach, B1 = man made, B2 = sandy beach, B3 = sandy beach and rocky coast, C1 = coastal waterway, C2 = coastal waterway and marsh, and C3 = tidal flat and sandy beach.

Figure 23. February 28, 2018, CRSB mosaic

THIS PAGE INTENTIONALLY LEFT BLANK

LIST OF REFERENCES

Al Bakri, D., 1996: Natural hazards of shoreline bluff erosion: A case study of Horizon View, Lake Heron. *Geomorphology*, **17**, 323–337.

Banda, J., R.A. Angryk, and P.C. Martens, 2013: Steps towards large-scale solar image data analysis to differentiate solar phenomena. *Solar Physics*, **288(1)**, 1–28.

Buscombe, D. and S.C Ritchie, 2018: Landscape classification with deep neural networks. *Geosciences*, **8**,(244), 1–23.

Cermakova, I., J. Komarkova, and P. Sedlak, 2016: Using UAV to detect shoreline changes: Case study—Pohranov Pond, Czech Republic. *Remote Sensing and Spatial Information Sciences*, **XLI-B1**, 803–808.

Chen, D. and D.A., Stow, 2002: The effect of training strategies on supervised classification at different spatial resolution. *Photogrammetric Engineering and Remote Sensing*, **68**, 1155–1162.

Chollett, F., 2018: Deep Learning with Python. Manning Publications Co., Shelter Island, NY. 361pp.

Costa, M.P.F., 2004: Use of SAR satellites for mapping zonation of vegetation communities in the Amazon floodplain. *Int. J. Remote Sensing*, **25**, 1817-1835.

Cracknell, A.P., 1998: Synergy in remote sensing—What's in a pixel? *International Journal of Remote Sensing*, **19**, 2025–2047.

d'Oleire-Oltmanns, S., I. Marzoff, K.D. Peter, and J.B. Ries, 2012: Unmanned aerial vehicle (UAV) for monitoring soil erosion in Morocco. *Remote Sensing*, **4**, 3390–3416.

Dunford, R., K. Michel, M. Gagnage, H. Piegay, and M.L. Tremelo, 2009: Potential and constraints of unmanned aerial vehicle technology for the characterization of Mediterranean riparian forest. *Int. J. Remote Sens.*, **30**, 4915–4935.

Fisher, P., 1997: The pixel: A snare and a delusion. *International Journal of Remote Sensing*, **18**, 679–685.

Gatys, L., A.S. Ecker, and M. Bethge, 2015: Texture synthesis using convolutional neural networks. *Advances in Neural Information Processing Systems 28 (NIPS 2015)*.

Ghosh, M.K., L. Kumar, and C. Roy, 2015: Monitoring the coastline change of Hatiya Island in Bangladesh using remote sensing techniques. *ISPRS Journal of Photogrammetry and Remote Sensing*, **101**, 137–144.

Han, S., H. Mao, and W.J. Dally, 2016: Deep compression: Compressing deep neural networks with pruning, trained quantization and Huffman coding. *ICLR* 2016.

Hubert-Moy, 2001: A comparison of parametric classification procedures of remotely sensed data applied on different landscape units. *Remote Sensing of Environment*, **75**, 174–187.

Hugenholtz, C.H., and K. Whitehead, 2014: Remote sensing of the environment with small unmanned aircraft systems (UASs), part 1: a review of progress and challenges. *J. Unmanned Veh. Syst.*, **2**, 69–85.

Hoonhut, B.M., M. Radermacher, F. Baart, and L.J.P. van der Maaten, 2015: An automated method for semantic classification of regions in coastal images. *Coastal Engineering*, **105**, 1–12.

Johnson, L.F., S. Herwitz, S. Dunagan, B. Lobitz, D. Sullivan, and R. Slye, 2003: Collection of ultra high spatial and spectral resolution image data over California vineyards with a small UAV. *Proceeding of the International Symposium on Remote Sensing of Environment*, Honolulu, HI, USA, 10-14 November 2003; p.3.

Joyce, K.E., S.E. Belliss, and S.V. Samsonov, 2009: A review of the status of satellite remote sensing and image processing techniques for mapping natural hazards and disasters. *Progress in Physical Geography*, **33(2)**, 183–207.

Kankara, R.S., S.C. Selvan, V.J. Markose, R. Bhoopathy, and S. Arockiaraj, 2015: Estimation of long and short term shoreline changes along Andhra Pradesh coast using remote sensing and GIS techniques. *Procedia Engineering*, **116**, 855–862.

Krizhevsky, I. Sutskever, and G.E. Hinton, 2012: Imagenet classification with deep convolutional neural networks. In *Advances in Neural Information Processing Systems*, pp.1097-1105.

Kubat, M., R.C. Holte, and S. Matwin, 1998: Machine Learning for the detection of oil spills in satellite radar images. *Machine Learning*, **30**, 195–215.

Kuleli, T., A. Guneroglu, F. Karsli, and M. Dihkan, 2011: Automatic detection of shoreline change on coastal Ramsar wetlands of Turkey. *Ocean Engineering*, **38**, 1141–1149.

Landgrebe, D.A., 2003: Signal Theory Methods in Multispectral Remote Sensing, Hoboken, NJ: John Wiley and Sons. 528pp.

Lelong, C.C. D., P. Burger, G. Jubelin, B. Roux, S. Labbe, and F. Baret, 2008: Assessment of unmanned aerial vehicles imagery for quantitative monitoring of wheat crop in small plots. *Sensors*, **8**, 3557–3585.

Li, A., and M.C.J. Damen, 2010: Coastline change detection with satellite remote sensing for environmental management of the Pearl River Estuary, China. *Journal of marine Systems,* **82**, S54-S61.

Lu, D., and Q. Weng, 2007: A survey of image classification methods and techniques for improving classification performance. *International Journal of Remote Sensing*, **28:5**, 823–870.

Maiti, S. and A.K. Bhattacharya, 2009: Shoreline change analysis and its application to prediction: A remote sensing and statistics based approach. *Marine Geology*, **257**, 11–23.

Marmanis, D., M. Datcu, T. Esch, and U. Stilla, 2015: Deep learning earth observation classification using ImageNet pretrained networks. *IEEE: Geoscience and Remote Sensing Letters, Vol. 13.* No. **1**, January 2016.

Mas, J.F., 2004: Mapping land use/cover in a tropical coastal area using satellite sensor data, GIS and artificial neural networks. *Estuarine, Coastal and Shelf Science*, **59**, 219–230.

Mather, P.M., 2004, Computer Processing of Remotely-Sensed Images: An Introduction, 3rd ed., Chichester: John Wiley & Sons, 442pp.

Mattis, J., 2018. *Summary of the National Defense Strategy 2018*. Washington, DC: Department of Defense. https://dod.defense.gov/Portals/1/Documents/pubs/2018-National-Defense-Strategy-Summary.pdf.

Natesan, U., A. Parthasarathy, R. Vishnunath, G. Edwin Jeba Kumar, and V.A. Ferrer, 2015: Monitoring long term shoreline changes along Tamil Nadu, India using geospatial techniques. *Aquatic Procedia*, **4**, 325–332.

NOAA. (2013). *Shoreline Assessment Manual.* U.S. Dept. of Commerce. Seattle, WA: Emergency Response Division, Office of Response and Restoration, National Oceanic and Atmospheric Administration, 73 pp + appendices.

Orescanin, M.M., and J. Scooler, 2018: Observations of episodic breaching and closure at an ephemeral river. *Continental Shelf Research*, **166**, 77–82.

Quora, 2018: What is the difference between neural networks and deep learning, Accessed October 2018, https://www.quora.com/What-is-the-difference-between-Neural-Networks-and-Deep-Learning

Rango, A., A.S. Laliberte, J.E. Herrick, C. Winters, K.M. Havstad, C. Steele, and D.M. Browning, 2009: Unmanned aerial vehicle-based remote sensing for rangeland assessment, monitoring, and management. *J. Appl. Remote Sens.*, **3**, 1–15

Scooler, J, 2017: Episodic changes in lagoon water levels due to ephemeral river breaching and closure events. M.S. Thesis, Dept. of Oceanography, Naval Postgraduate School, 47pp.

Sherman, D.J. and B.O. Bauer, 1993: Coastal morphology through the looking glass. *Geomorphology*, **7**, 225–249.

Simonyan, K. and A. Zisserman, 2014: Very deep convolutional networks for large-scale image recognition. *ICLR* 2015.

Tamassoki, E., H. Amiri, and Z. Soleymani, 2014: Monitoring of shoreline changes using remote sensing (case study: coastal city of Banddar Abbas). *IOP Conf. Series: Earth and Environmental Science*, **20**, 1–7.

Turner, D., A. Lucieer, and C. Watson, 2012: An automated techniques for generating georectified mosaics from ultra-high resolution unmanned aerial vehicle (UAV) imagery, based on structure from motion (SfM) point clouds. *Remote Sens.*, **4**, 1392–1410.

Whitehead, K. and Coauthors, 2014: Remote sensing of the environment with small unmanned aircraft systems (UASs), part 2: scientific and commercial applications. *J. Unmanned Veh. Syst.* **2**, 86–102.

Xie, Y, Z. Sha, and M. Yu, 2008: Remote sensing imagery in vegetation mapping: A review. *Journal of Plant Ecology*, **1**, 9–23.

Young, W., 2018: Sediment transport associated with ephemeral river breaching and closing events. M.S. Thesis, Dept. of Oceanography, Naval Postgraduate School, 53pp.

INITIAL DISTRIBUTION LIST

1. Defense Technical Information Center
   Ft. Belvoir, Virginia

2. Dudley Knox Library
   Naval Postgraduate School
   Monterey, California